

# MRI based biomarker for brain aging in rodents and non-human primates

Katja Franke<sup>a</sup>, Robert Dahnke<sup>a</sup>, Geoffrey Clarke<sup>b</sup>, Anderson Kuo<sup>b</sup>, Cun Li<sup>c,d</sup>, Peter Nathanielsz<sup>c,d</sup>,

Matthias Schwab<sup>a</sup>, Christian Gaser<sup>a,c</sup>

<sup>a</sup> Department of Neurology, University Hospital Jena, Jena, Germany

<sup>b</sup> Radiology, University of Texas Health Science Center San Antonio, San Antonio, TX, United States.

<sup>c</sup> Texas Pregnancy & Life Course Health Research Center, Southwest National Primate Research Center, Texas Biomedical Research Institute, San Antonio, TX, United States.

<sup>d</sup> Animal Science, University of Wyoming, Laramie, WY, United States.

<sup>e</sup> Department of Psychiatry, University Hospital Jena, Jena, Germany

Corresponding author: [katja.franke@uni-jena.de](mailto:katja.franke@uni-jena.de)

**Abstract**—This work presents two novel species-specific adaptations of a MRI based biomarker that indicates individual deviations from normal brain aging trajectories for rodents and non-human primates. By employing automatic, species-specific preprocessing of anatomical brain MRI as well as high-dimensional pattern recognition methods, this approach uses the distribution of healthy brain-aging patterns to estimate individual brain ages. This biomarker may probably enable tracking the effects of developmental and environmental influences, manipulations, and (preventive) treatments on individual deviations from species-specific brain aging trajectories in experimental mammal models across the life-course.

**Keywords:** Aging; BrainAGE; DBM; MRI; relevance vector regression (RVR); machine learning; mammals; VBM

## I. INTRODUCTION

With the use of magnetic resonance imaging (MRI), cross-sectional as well as longitudinal neuroimaging studies are contributing to a better understanding of healthy as well as pathological neuroanatomical changes across the lifespan. Though neuroanatomical maturation and aging is characterized by a widespread but rather specific pattern of progressive and regressive alterations [1, 2], multiple factors affect and modify those individual trajectories. To study and quantify those individual deviations in humans, several MRI-based biomarkers using pattern recognition techniques were recently developed [3-6]. Applying those biomarkers, a big variety of factors were already found to be related to individual deviations from healthy brain aging in humans, e.g. several health and lifestyle factors [7]. However, experimental animal studies are mandatory to study the individual causes of deviations from healthy brain aging and to quantify their impact on individual brain aging trajectories. Therefore, species-specific MRI-based biomarkers for brain aging are needed to model brain aging and to indicate individual deviations from healthy brain aging trajectories in experimental studies with mammals.

Based on our well-established pattern recognition framework for individual brain aging in humans [3, 7, 8], this study presents two species-specific adaptations of the *BrainAGE* approach for non-human primates (baboons) and rodents (rats), including novel species-specific preprocessing pipelines for anatomical MRI data. Additionally, the study includes longitudinal analyses of individual brain aging trajectories in rodents.

## II. METHODS

### A. Samples

#### 1) Non-human primates

The sample of non-human primates included 29 [14 male] healthy control subjects (*Papio hamadryas*), aged 4–22 years [mean  $9.5 \pm 4.9$ y]. Each subject was scanned once on a 3T whole body scanner (TIM Trio, Siemens Medical Solutions, Malvern, PA) using a T1-weighted sequence. All animal procedures were performed in accordance with accepted standards of humane animal care approved by the Texas Biomedical Research Institute and University of Texas Health Science Center at San Antonio Institutional Animal Care and Use Committee and conducted in facilities approved by Association for Assessment and Accreditation of Laboratory Animal Care International Inc.

#### 2) Rodents

The sample of rodents included 24 control subjects without any treatments. Mean life span was  $734 \pm 110$  days. Subjects were scanned up to 13 times on a clinical 3T whole body Scanner (Magnetom TIM Trio, Siemens Medical Solutions, Erlangen, Germany), with rats being anesthetized during scanning session. In total, the sample included 273 MRI data sets (Table 1). A dedicated rat head coil with a linearly polarized Litz coil volume resonator design (Doty Scientific Inc., Columbia, SC, USA) was used in order to acquire T2-weighted images with an isotropic voxel size of 0.33 mm (matrix  $192 \times 130 \times 96$ , FoV  $64 \times 43 \times 32$  mm, bandwidth 145 Hz/px, TE/TR = 352 ms/2500 ms, flip angle mode ‘T2var’, echo spacing of 10.7ms, turbo factor of 67 and Partial Fourier of 7/8 in both phase encode directions).

### B. Basic concept of the brain age estimation framework

The brain age estimation framework (*BrainAGE*) was developed to model healthy brain aging in humans [3]. Its basic

TABLE I. CHARACTERISTICS OF THE RODENT SAMPLE

	Time point of MR scanning (number of day after birth)												
	97	104	118	146	174	258	342	426	510	594	678	762	846
No. MRI scans	24	24	24	24	24	24	23	23	23	23	20	9	8
MAE of brain age (days)	37	26	28	20	23	39	49	54	56	61	72	155	185
RMSE of brain age (days)	44	32	32	26	29	48	58	64	69	82	92	171	199

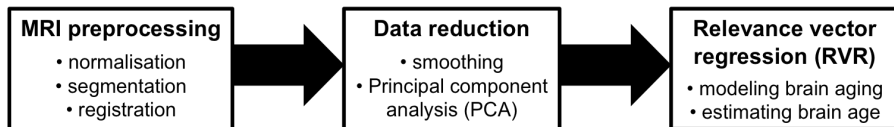


**Figure 1.** General flowchart of the brain age estimation framework.

concept is the aggregation of the complex, multi-dimensional aging pattern across the whole brain into one single value, i.e. the estimated brain age. In human samples, the *Brain-AGE* framework has been shown to accurately and reliably estimate the age of individual brains using structural MRI with minimal preprocessing and parameter optimization and also proved its potential to identify pathological brain aging on an individual level [3, 8].

In general, the workflow includes three steps (Fig. 1). First, the raw structural MRI data are preprocessed with a standardized voxel-based morphometry (VBM) pipeline in order to make them comparable and processable for the following analysis steps. Second, data reduction is performed via principal component analysis (PCA) on the preprocessed MRI data in order to reduce computational costs, to avoid severe overfitting, as well as to get a robust and widely applicable age estimation model. PCA is performed on the training data only and resulting transformation parameters are subsequently applied to the test sample. Third, relevance vector regression [RVR; 9] is utilized to capture the multidimensional aging patterns across the whole brain in order to model brain aging over a wide age range and to subsequently estimate individual brain ages.

In the present study, the original brain age estimation framework was adapted to build species-specific brain aging models for non-human primates and rodents, including newly developed species-specific preprocessing pipelines for anatomical MRI data.

### C. Preprocessing of MRI data

#### 1) Non-human primates

First, a slice-based inhomogeneity correction was used to remove MR protocol depending slice artifacts (Fig. 2a) [10, 11]. Then, a spatial adaptive non-local means filter (SANLM) [12] was applied to reduce high-frequency noise. For segmentation and spatial registration a baboon tissue probability map (TPM) and a Dartel template were required. The template was created in an iterative process based on a rescaled human template (Fig. 2b). For initialization, an affine transformation was used to scale the human SPM12 TPM and the CAT12 Dartel template map to the expected

brain size of baboons (i.e., ~140ml vs. ~1400ml in humans). Image resolution of the template was changed to isotropic voxel size of 0.75mm. For each iteration step, the resulting tissue maps were averaged and smoothed

with a full-width-at-half-maximum (FWHM) kernel of 2mm to estimate an affine registration in order to create a new TPM, T1 average map and brainmask. For averaging data, the median function was used to reduce distortions by outliers and failed processing. Iterations were stopped if the change compared to the previous template was below a pre-defined threshold, resulting in final segmentation (Fig. 2c).

#### 2) Rodents

To automatically preprocess and analyze MRI of rats, a preprocessing framework including several realignment and normalization steps was utilized, providing analysis in the space of Paxinos atlas [13]. First, an initial affine co-registration to the Paxinos template using normalized mutual information was applied. In the next step all time points of one data set were registered to the baseline scan and deformations between all time points and the baseline were estimated. This deformation based morphometry (DBM) approach is a useful technique to detect structural differences over the entire brain since it analyzes positional differences between every voxel and a reference brain. After this non-linear registration, the morphological differences between both brains are minimized and the deformations now encode information about these differences. The Jacobian determinant can be finally used to calculate local volume changes at every voxel.

### D. Data reduction

#### 1) Non-human primates

Preprocessed MRI data were smoothed with a 3mm FWHM smoothing kernel. Images were resampled to 3mm.

#### 2) Rodents

After species-specific MRI preprocessing, the resulting Jacobians in each voxel were filtered with a smoothing kernel comparable to a 4mm FWHM smoothing kernel normally used for human data.

### E. Species-specific brain age estimation framework

The brain age estimation framework utilizes RVR with a linear kernel because of former results in human data indicating favorable performance of RVR to capture the typical age-

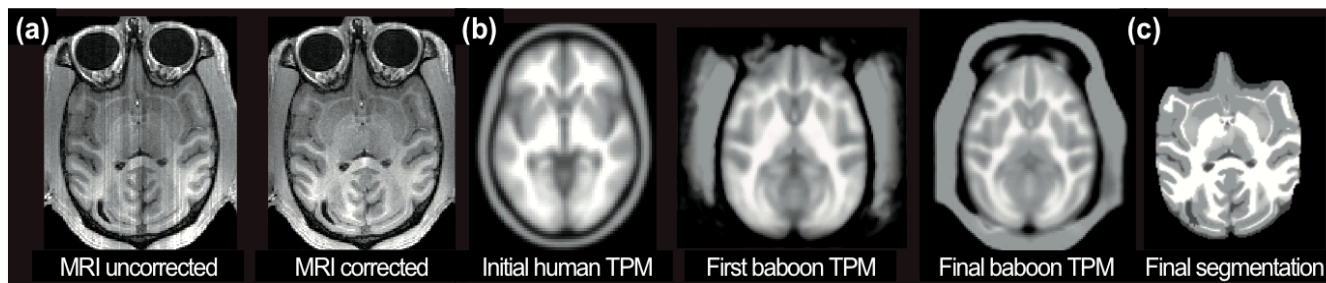


**Figure 2.** Preprocessing pipeline for baboon MRI. (a) Slice-based inhomogeneity correction was performed to remove MR protocol dependent slice artifacts. (b) For segmentation and spatial registration, a baboon tissue probability map (TPM; shown as label map) was created in an iterative refinement process based on a rescaled human template (left). (c) The final TPM was used for final segmentation of anatomical MRI.

specific atrophy patterns across the whole brain. Additionally, age estimation accuracy was not improving when choosing non-linear kernels [3]. Besides and in contrast to support vector machines, parameter optimization via cross-validation during the training procedure is not necessary as this is automatically performed within the algorithm itself [9]. In general, the model is trained with preprocessed whole brain structural MRI data and corresponding chronological ages of a training sample, resulting in a complex model of brain aging. Put in other words, the algorithm uses those data sets from the training sample that represent the prototypical examples within the specified regression task (i.e., brain aging). Voxel-specific weights are calculated that represent the contribution of each voxel within the specified regression task (i.e., brain aging). Subsequently, the brain age of a new test subject can be calculated by applying the weights-vector to the individual preprocessed MRI data, aggregating the complex, multidimensional aging pattern across the whole brain into one single value. The difference between estimated brain age and chronological age reveals the individual deviation score, namely the brain age gap estimation (*BrainAGE*) score. Consequently, positive or negative values of this deviation score directly quantify the amount of acceleration or delay in individual brain aging, respectively.

#### 1) Non-human primates

For baboons, only the gray matter images are used to build the model of brain aging in baboons. The brain age estimation model was trained and tested via leave-one-out (LOO). PCA was repeatedly performed on the training data and subsequently applied to the test data before RVR inside each LOO loop.

#### 2) Rodents

For rats, training and testing of the brain age estimation model was done performing subject-specific LOO. In detail, the brain age estimation model was trained performing RVR with the preprocessed whole brain structural MRI data from all scanning time points of 23 out of a total of 24 subjects to model the neuroanatomical aging process. Subsequently, the individual brain age at each scanning time point of the left-out test subject was estimated using its corresponding MRI data. PCA was repeatedly performed on the training data and subsequently applied to the test data before RVR inside each LOO loop. The whole procedure was repeated 24 times.

#### F. Technical notes

The whole brain age estimation framework works fully automatically. All MRI preprocessing, data reduction, model training, and brain age estimation was done using MATLAB. For preprocessing the T1-weighted images SPM8 was used ([www.fil.ion.ucl.ac.uk/spm/](http://www.fil.ion.ucl.ac.uk/spm/)), integrating our new CAT12 toolbox (<http://dbm.neuro.uni-jena.de>). The ‘Matlab Toolbox for Dimensionality Reduction’ (<http://ict.ewi.tudelft.nl/~lvandermaaten/Home.html>) was used for PCA. ‘The Spider’ ([www.kyb.mpg.de/bs/people/spider/main.html](http://www.kyb.mpg.de/bs/people/spider/main.html)) was used to perform RVR.

Baboon TPM and template generation takes around 30 minutes per subject and iteration, ending up in about 2 days for the whole sample. The full description of the TPM, template and atlas generation process is actually prepared for a

separate publication. For the sample including 29 baboons with one MRI data set per subject, the whole process of training the baboon-specific *BrainAGE* model and estimating the individual brain ages takes about 20 sec in total. Preprocessing MRI data of the rodents takes about 10–15 min per MRI data set on MAC OS X, Version 10.6.3, 2.8 GHz Intel Core 2 Duo. For the sample including 24 rats with up to 13 MRI data sets per subject, the whole process of training the rodent-specific *BrainAGE* model and estimating the individual brain ages takes about 285 sec in total.

#### G. Statistical analysis

To measure the accuracy of the age estimation, the correlation coefficient, mean absolute error (MAE), and root mean squared error (RMSE) between chronological age and estimated brain age were calculated:

$$\text{MAE} = 1/n * \sum_i |BA_i - CA_i|, \quad (1)$$

$$\text{RMSE} = [1/n * \sum_i (BA_i - CA_i)^2]^{1/2}, \quad (2)$$

with  $n$  being the number of subjects in the test sample,  $BA_i$  being the estimated brain age, and  $CA_i$  being the chronological age.  $F$  statistics of linear and quadratic regression models were used to analyze best-fit between BA and CA. Multivariate linear regression was used to analyze the individual brain aging trajectories over lifespan in rats. All statistical testing was performed using MATLAB.

### III. RESULTS

#### A. Performance of the BrainAGE model in baboons

With a correlation of  $r=0.80$  ( $p<0.0001$ ) to the chronological, estimation of brain ages from anatomical MRI scans in the baboon sample showed very good accuracy. MAE was 2.1y, which equates to an age estimation error of 11% in relation to the age ranged used in this study. The linear regression model showed the best fit between chronological and estimated age ( $R^2=0.64$ ;  $F=47.5$ ;  $p<0.0001$ ; Fig. 3) as compared to the quadratic fit ( $R^2=0.64$ ;  $F=23.0$ ;  $p<0.0001$ ).

#### B. Performance of the BrainAGE model in rodents

Brain age estimation was highly accurate in the sample of rats ( $r=0.95$ ;  $p<0.0001$ ). Mean MAE was 49d, which equates

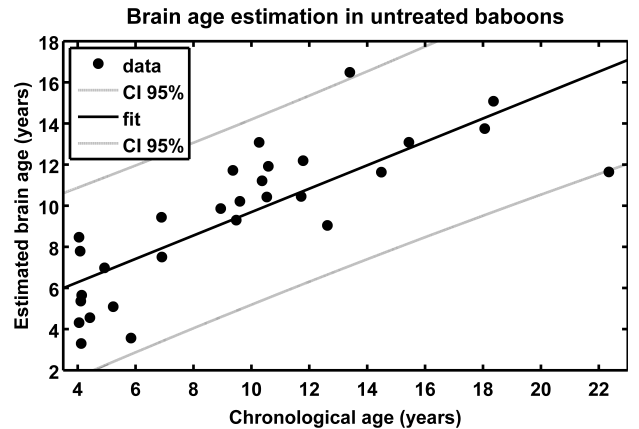


**Figure 3:** Chronological and estimated brain ages are shown for the sample of healthy control baboons, including the 95% confidence interval (gray lines). Correlation between chronological and estimated brain age was  $r=0.80$  ( $p < 0.0001$ ).

to an age estimation error of 6% in relation to the age ranged used. Mean RMSE was 71d. Individual MAEs and RMSEs for each single scanning time point can be found in Table 1. The linear regression model showed a slightly better fit between chronological and estimated age ( $R^2=0.91$ ;  $F=2622.3$ ;  $p<0.0001$ ; Fig. 4a) than the quadratic fit ( $R^2=0.91$ ;  $F=1309.8$ ;  $p<0.0001$ ). Longitudinal analyses of individual brain aging trajectories showed more variance at old ages (Fig. 4b).

#### IV. DISCUSSION

For brain age estimation in mammals based on anatomical brain MRIs, this study proposes species-specific adaptations of the fast and fully automatic brain age estimation framework originally developed for the use with human brain MRI data [3], including the development of new preprocessing pipelines for anatomical MRI data of rodents and non-human primates. Using about 270 MRI data, the rodent-specific *BrainAGE* method showed excellent performances, explaining 91% of the individual variations in brain structures. As shown in the human *BrainAGE* study, the number of training subjects has the strongest influence on age prediction accuracy – above the choice of preprocessing method, regression kernel or pattern recognition algorithm [3]. With only 29 MRI data in the baboon sample, the baboon-specific brain age estimation framework showed very good performance, but will certainly improve when adding additional data. As already shown in human studies, several factors are influencing individual brain aging trajectories [7]. Implementing these novel species-specific MRI-based biomarkers for brain aging in mammals, future studies may probably track the effects of a variety of experimental manipulations on individual cerebral atrophy. In conclusion, the *BrainAGE* biomarker could potentially help to recognize and indicate a variety of environmental factors that cause advanced brain atrophy on an individual level in epidemiological as well as experimental animal studies, thus finally contributing to a better understanding of healthy and pathological brain aging.

#### ACKNOWLEDGMENT

This work was supported in part by the European Community [FP7 HEALTH, Project 279281 (BrainAge)], NIH K25 DK089012,

and NIH R24 RR021367.

#### REFERENCES

- [1] C. D. Good, I. S. Johnsrude, J. Ashburner, R. N. Henson, K. J. Friston, and R. S. Frackowiak, "A voxel-based morphometric study of ageing in 465 normal adult human brains," *NeuroImage*, vol. 14, pp. 21-36, 2001.
- [2] T. J. Silk and A. G. Wood, "Lessons about neurodevelopment from anatomical magnetic resonance imaging," *Journal of Developmental & Behavioral Pediatrics*, vol. 32, pp. 158-168, 2011.
- [3] K. Franke, G. Ziegler, S. Klöppel, C. Gaser, and the Alzheimer's Disease Neuroimaging Initiative, "Estimating the age of healthy subjects from T1-weighted MRI scans using kernel methods: Exploring the influence of various parameters," *NeuroImage*, vol. 50, pp. 883-892, 2010.
- [4] D. Tosun, P. Mojabi, M. W. Weiner, and N. Schuff, "Joint analysis of structural and perfusion MRI for cognitive assessment and classification of Alzheimer's disease and normal aging," *NeuroImage*, vol. 52, pp. 186-197, 2010.
- [5] B. Wang and T. D. Pham, "MRI-based age prediction using hidden Markov models," *J Neurosci Methods*, vol. 199, pp. 140-145, 2011.
- [6] Y. Wang, Y. Fan, P. Bhatt, and C. Davatzikos, "High-dimensional pattern regression using machine learning: from medical images to continuous clinical variables," *NeuroImage*, vol. 50, pp. 1519-1535, 2010.
- [7] K. Franke, M. Ristow, and C. Gaser, "Gender-specific impact of personal health parameters on individual brain aging in cognitively unimpaired elderly subjects," *Frontiers in aging neuroscience*, vol. 6, p. 94, 2014.
- [8] K. Franke, C. Gaser, for the Alzheimer's Disease Neuroimaging Initiative, "Longitudinal changes in individual *BrainAGE* in healthy aging, mild cognitive impairment, and Alzheimer's disease," *GeroPsych: The Journal of Gerontopsychology and Geriatric Psychiatry*, vol. 25, pp. 235 - 245, 2012.
- [9] M. E. Tipping, "Sparse bayesian learning and the relevance vector machine," *Journal of Machine Learning Research*, vol. 1, pp. 211-244, 2001.
- [10] M. S. Cohen, R. M. DuBois, and M. M. Zeineh, "Rapid and effective correction of RF inhomogeneity for high field magnetic resonance imaging," *Hum Brain Mapp*, vol. 10, pp. 204-211, 2000.
- [11] K. Van Leemput, F. Maes, D. Vandermeulen, and P. Suetens, "Automated model-based bias field correction of MR images of the brain," *IEEE Trans Med Imaging*, vol. 18, pp. 885-896, 1999.
- [12] P. Christidis and A. Cox, "Step-by-Step Guide to Cortical Surface Modeling of the Nonhuman Primate Brain Using FreeSurfer," in *Human Brain Mapping Annual Meeting*, 2006.
- [13] C. Gaser, S. Schmidt, M. Metzler, K. H. Herrmann, I. Krumbein, J. R. Reichenbach, et al., "Deformation-based brain morphometry in rats," *NeuroImage*, vol. 63, pp. 47-53, 2012.

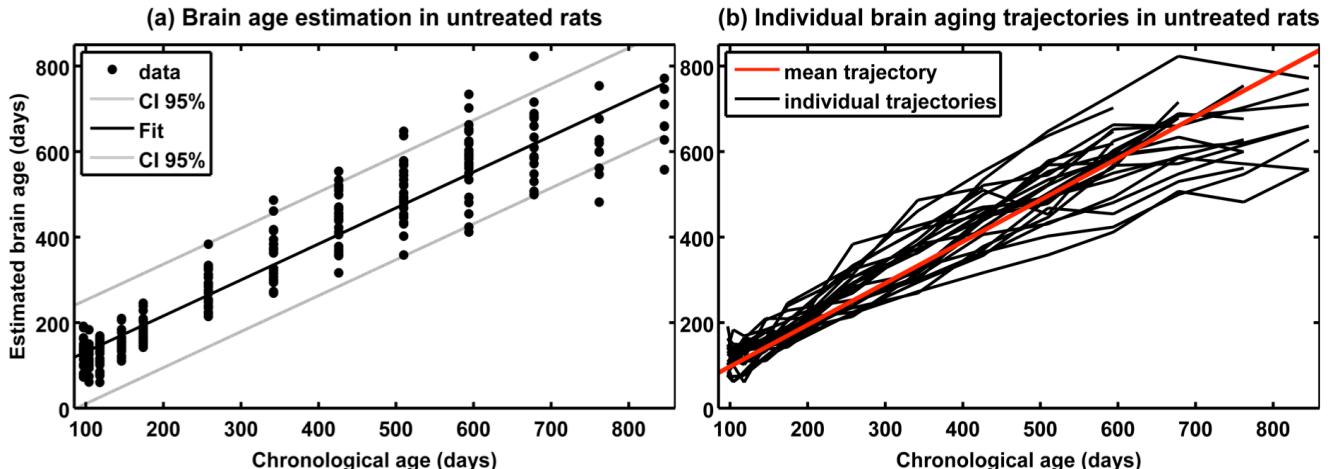


**Figure 4.** (a) Chronological and estimated brain age are shown for the sample of untreated control rats, including the 95% confidence interval (gray lines). The overall correlation between chronological and estimated brain age was  $r=0.95$  ( $p < 0.0001$ ). (b) Longitudinal brain aging trajectories.